Detecting and Mapping the Urban Heat Island in a Small South Texas City

Brent C. Hedquist[1] and Cody Barker[2]*

[1]*Department of Physics & Geosciences, Texas A&M University-Kingsville , Kingsville, TX, 78363 USA*

[2]*American Shoreline, Inc., Corpus Christi, TX 78401 USA*

**Corresponding author:* Email: brent.hedquist@tamuk.edu

Abstract

In this study, field measurements, GIS, and remote sensing techniques, were used to detect and map the urban heat island (UHI) effect in the city of Kingsville, Texas during spring 2013. Field measurements of temperature and humidity were collected using a small network of fixed weather sensors and mobile measurements. Additional surface temperature measurements were acquired from satellite sensor datasets. Spatial interpolation in GIS was employed to analyze temperature patterns across the city. A peak UHI of 3.6°C was detected during a field experiment in late March. It was located between the downtown and the northern periphery of the city. The downtown typically experienced a "cool island," similar to what is found in much larger urban areas like Phoenix or Houston, during late-morning and early-afternoon periods. Remotely-sensed satellite data revealed a reversal of the UHI within unplanted (fallow) and dry agricultural fields in the immediate vicinity of Kingsville, as land-surface temperatures were several degrees warmer than in the downtown area during the late morning. Higher temperatures detected were most likely due to the absence of vegetation and shade, as well as reflecting low soil-moisture stemming from a several years-long drought in the region. These results may be important for the climate-change and excessive-heat management strategies of both farmers and managers in the city of Kingsville. In light of these results, heat mitigation strategies, including tree cover and crop planting techniques to reduce bare soil, should be considered.

Key words: urban microclimates, urban heat island, South Texas, thermal remote sensing

1. Introduction

The urban heat island (UHI) effect is a well-studied phenomenon in which urban areas typically attain higher temperatures, especially at night, due to the engineered (built) environment (i.e., surface materials such as asphalt, brick and concrete, and the heat trapping effects of buildings), compared to the wide-open vegetated spaces of surrounding rural areas (Oke 1987; Chow, Brennan, and Brazel 2012). The majority of UHI studies have focused on large, mid-latitude cities, while less research has been conducted on UHIs of small- to mid-sized cities (Arnfield 2003). The magnitude of the UHI is directly related to city size, with larger cities experiencing the highest magnitudes (Oke 1973). The UHI typically forms as urban landscapes absorb solar radiation and heat is trapped within the higher density of buildings. Urban surfaces such as those covered in asphalt and concrete absorb more solar energy and reradiate heat more slowly than do surfaces in rural areas. A greater amount of heat is retained in the late afternoon and early evening by the city's surfaces rather than being released quickly as happens in rural, naturally vegetated areas. In general, the greatest UHI (temperature contrast magnitude) between urban and rural areas occurs 3-5 hours after sunset (Oke 1987; Geiger, Aron, and Todhunter 2003). Within arid environments, the microclimate variation in a city is found to be directly related to the land cover and amount of vegetation (Stabler, Martin, and Brazel 2005).

In addition to city size, change in the maximum urban heat island, or ΔTu-r(max), is found to be directly related to wind speed and cloud cover (Unger, Sumeghy, and Zoboki 2001). Cloudy skies (mainly lower atmospheric stratus-type clouds), as well as higher wind speeds (> 4 m s-1), tend to dramatically decrease the intensity of the UHI effects (Oke 1987; Unger, Sumeghy, and Zoboki 2001).

Higher wind speeds tend to mix the air in the lower atmosphere within cities and minimize any urban-rural temperature differences. Due to this, the optimal equation, explaining the greatest variance in the maximum heat island and including the average wind speed is:

$$\Delta T_{u\text{-}r}(max) = 1.91 \log P - 2.07\ u1/2 - 1.73 \qquad (1)$$

Where P is population and u average wind speed (Oke, 1973)

In arid and semi-arid environments, the UHI tends to amplify during strong anti-cyclonic events, especially when combined with low humidity and dry soil conditions. Hedquist (2005) measured a UHI magnitude as high as 4.7°C during a spring day experiencing warmer and drier than average conditions, as well as light winds, within the city of Casa Grande, Arizona. Casa Grande is approximately 70 km southeast of Phoenix, Arizona and had a population estimated at 31,000 in 2004. The high magnitude of this event (comparable to much larger cities) was most likely due to strong radiative differences between the surfaces of the built environment and the surrounding rural areas due to the light winds (Goward 1981; Oke 1982; Hedquist 2002).

The UHI phenomenon can be categorized by scale within various atmospheric boundary layers, such as the meso-scale urban boundary layer or the urban canopy layer, which reflects temperature differences near the ground at more local (i.e. larger) scales (Oke 1976), or by regarding the existence of surface temperature differences (surface UHI). The majority of empirical studies on the UHI have focused on the urban canopy layer (UCL). Within the UCL, the UHI has been traditionally measured using both *in situ* and mobile methods (Arnfield 2003; Sun et al. 2010; Chow, Brennan, and Brazel 2012). More recently, remote sensing of the UHI has become more common, especially with improvements and advancements that have been made to sensor technology. The surface UHI (SUHI) has been accurately measured by both IR thermography, satellite, and other remote sensing techniques (Aniello et al. 1995; Saaroni et al. 2000; Voogt and Oke 2003; Hedquist, 2010).

Heat-reduction strategies and UHI mitigation techniques have become a larger focus of international urban climate research in recent years, supporting advocacy for the use of cool roofs, permeable pavements, better building design, and urban forestry to reduce cooling demand, pollution, and human discomfort. Cool roofs include the use of reflective paints and materials as well as construction of green roofs to reduce energy demand (Georgescu et al. 2014; Middel, Chetri, and Quay 2015). The use of urban forestry as a UHI mitigation technique has been strongly advocated for cities around the world, especially in humid subtropical locations. In Texas, Sung (2013) found that land surface temperatures (LST) of a heavily-treed suburb of Houston, The Woodlands, were on average 1.5 - 3.9°C cooler than neighborhoods that lacked trees due to missing tree protection policies. The benefits of tree planting and effective urban forestry programs are well known. Trees, once established, mitigate not only heating due to evapotranspiration and shading effects, but also control pollution, reduce soil erosion, increase energy efficiency, and increase human comfort and health (Debbage and Shepherd 2015; Texas Trees Foundation 2014).

The objective of this study is to describe the spatial patterns of the UHI and the microclimate in Kingsville, Texas, a small subtropical south Texas city. The methods used in this research are modeled on a study done by Hedquist (2005) in Casa Grande, Arizona, a similarly sized city. The results are interpreted to provide city planners and policy makers with advice about heat-mitigation measures (such as urban forestry techniques, strategic tree planting, creation and maintenance of green and open spaces) that could be used in the region.

2. Methodology

2.1. Study area

Kingsville, Texas is located in southern Texas (27°31'N, 97°52'W), approximately 50 km southwest of Corpus Christi, Texas and 50 km west of the Gulf of Mexico. The most recent U.S. Census Bureau population estimate in 2014 is 26,529 (U.S. Census, 2016). The city is geographically part of the Texas Coastal Bend region, an area of relatively flat, coastal plain that extends from the Texas-Louisiana border in the east, to Brownsville, at the Mexican border, in the south (Figure 1). The elevation is close to sea level at 20 m and does not vary by more than 5 m across the city, with terrain changes confined to river courses and drainage systems. The city was founded in 1904 as a railroad town and is named for the King Ranch (founded in 1853), one of the largest and most well-known ranches in the United States.

Kingsville is located in a climatological transition area between the Chihuahuan Desert to its west, and the humid subtropics to its east. With a low-latitude location near the Tropic of Cancer (similar to central Florida), the city experiences a relatively high annual average temperature of 22.6°C (72.7°F), with an average annual rainfall of 700 mm (27 in), (NCDC 2014) as reflected in a climograph of monthly average temperature and precipitation (1981-2010) at the Kingsville Naval Air Station (KNQI) (Figure 2). The moderate annual rainfall total and a mild winter result in a climate classification of humid subtropical. However, due to extensive dry periods and high evapotranspiration rates, the vegetation is more brush-like, consisting of mesquite trees, occasional oak trees, and a mixture of drought-tolerant plants. Thus, the climate during dry times of the year appears to be more typical of semi-arid tropical grasslands than those found in humid tropical climates due to the higher frequency of extensive periods of warmer temperatures and dry conditions experienced in South Texas.

2.2. Data Acquisition

Data were acquired from several different sources: fixed weather station data, mobile-device measurements, and remotely sensed data archives. The fixed weather stations consisted of ten HOBO Pro data logger temperature and humidity sensors from Onset Computer Corporation. The data loggers were deployed for approximately five weeks, from late March to early May 2013. Data were recorded at 5 min intervals, 24 hours per day and then downloaded and extracted into

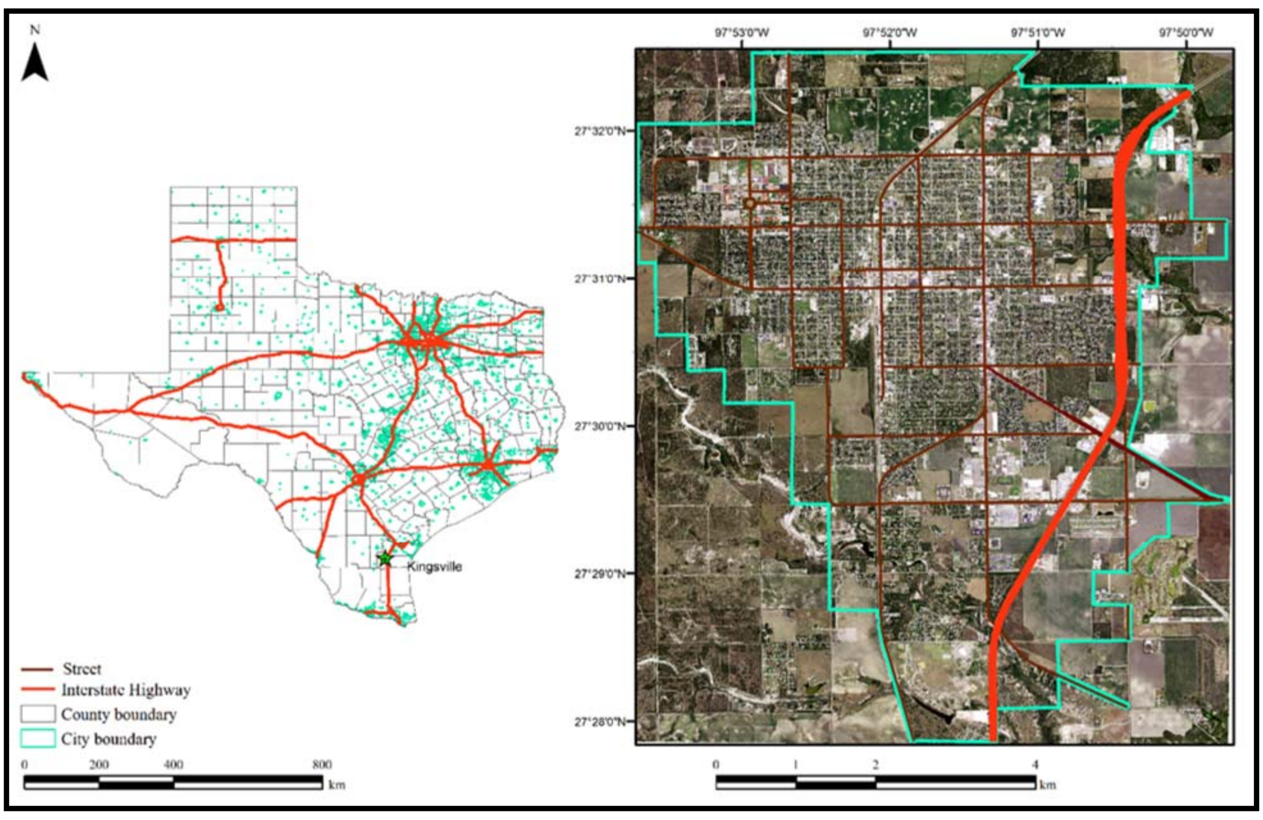

Figure 1. Kingsville, Texas study area map showing location in Texas, city boundaries, and major roads

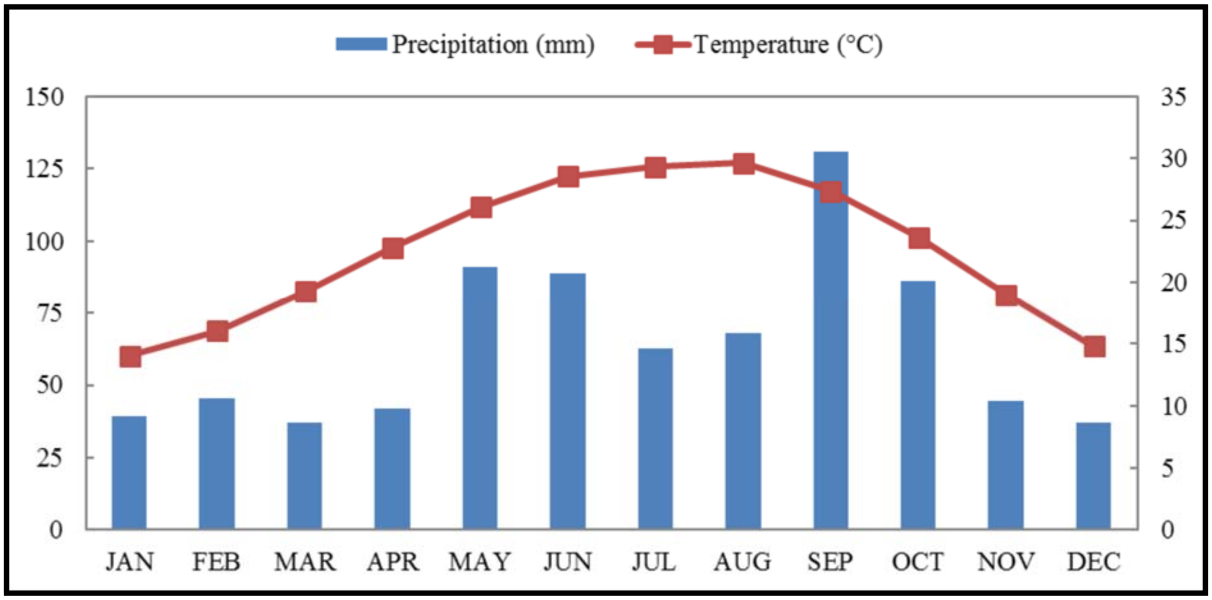

Figure 2. Monthly climate normals (1981-2010) for Kingsville, Texas (KNQI). Data were obtained from http://ncdc.noaa.gov/cdo-web/datatools/normals.

Microsoft Excel for analysis. Prior to deployment, data loggers were calibrated and found to have acceptable margins of error of + 0.1°C and + 1% RH.

Data loggers were deployed at eight representative urban sites and two rural sites throughout the urban region at 2.5 m (Figure 3). Representative sites were defined as locations that possessed similar characteristics to surrounding land cover within ~500 m. For example, the urban sites selected in the study were next to roadways and were surrounded by urban land covers that also included structures, whereas the rural sites were at grass-covered locations surrounded by areas of grass, trees, and other vegetation, but few buildings. Data logger heights were placed to avoid tampering with and or vandalism of the equipment during the five-week deployment. The placement of the majority of the loggers was on metal light posts less than 2 m from the street at various local businesses. Prior to deployment, permission was obtained from local businesses to mount the equipment on their respective properties, as legal policy of the regional power company restricted our use of utility poles for logger placement. Since the data loggers did not include wind measurement, hourly wind speed and direction measurements as well as cloud cover information were obtained from the Kingsville Naval Air Station (KNQI) monitors via the Weather Underground archived data website (https://www.wunderground.com/history/airport/KNQI/). KNQI is an Automated Surface Observing Station (ASOS) operated by the U.S. Navy and is located ~5 km southeast of downtown Kingsville (27°30'N, 97°49'W, 15 m elevation).

During the latter part of the study period, mobile transects were conducted throughout Kingsville in an automobile to collect high resolution temperature and humidity data. Vehicle-mounted sensors included a Campbell Scientific HMP60 temperature and relative humidity probe, SI-111 precision infrared radiometer for surface road temperature measurements, and a magnetically mounted Garmin GPS16X-HVS GPS receiver (Figure 4). A Campbell Scientific CR850 data logger collected and stored readings. Mobile equipment had been calibrated with HOBO data loggers two weeks prior to data collection in March 2013. Observations and data collection were conducted on two evenings (25 April and 1 May), and data were recorded every sec. The limited number of sampling days was due to technical difficulties during the study period. Prior to data collection, an optimal mobile sampling route was planned to collect the best samples of urban and rural areas of the city within vicinity of the HOBO weather sensors (Figure 3). In addition, the route was carefully plotted and intentionally limited so as to complete it in less than 30 min to reduce temperature biases that might occur from normal daytime heating or cooling. Due to the low number of samples and inconclusive results from the GIS data analysis of temperature readings, the results from mobile transects are not discussed in this paper.

In addition to mobile and stationary measurements, remote sensing data were used to track

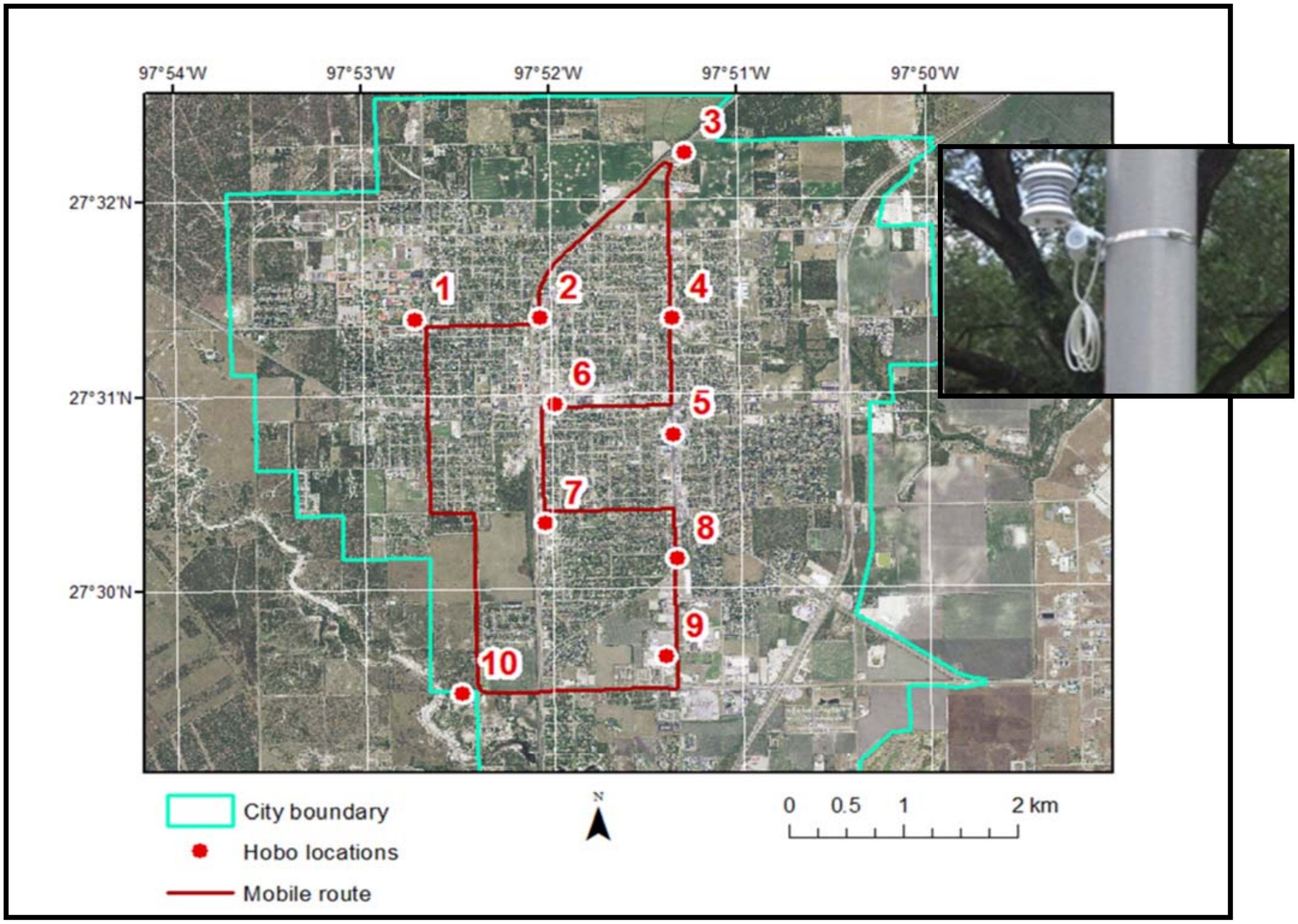

Figure 3. Fixed station (HOBO) locations and mobile sampling route located within the city of Kingsville. The mobile route was traveled in a clockwise direction with a start and finish at Hobo #1. Inset, upper right, illustrates HOBO sensor set-up on a pole 2.5 m off the ground. HOBO #6 is the approximate location of downtown Kingsville. KNQI is not shown, but is located just off the far right border of the map.

surface temperature within Kingsville prior to, during, and immediately after the March-May 2013 study period. Data from both ASTER/Terra (90 m resolution) and Landsat 8 (100 m resolution) were acquired from the USGS Earth Explorer website (earthexplorer.usgs.gov), as well as NASA/JPL. While the Landsat 8 images were freely available through the USGS Earth Explorer website, requests for ASTER imagery was obtained from the Japanese team managing the ASTER/Terra satellite sensor, which was subsequently approved for priority mission requests with orbit data acquisitions near Kingsville during the study period (April through May 2013). Unfortunately, data acquired of the Kingsville area was unusable due to cloud cover contamination on all of the days requested. As a result, we were forced to acquire an image from the imagery archives from November 2012 as this was the period closest to the study period that provided cloud-free thermal IR imagery.

2.3. GIS mapping and interpolation

ESRI's ArcGIS 10.1 GIS software was utilized to map and identify microclimatic variations in surface and near-ground air temperatures within Kingsville during the spring 2013 study period. Within ArcGIS, the Spatial Analyst extension was used to create spatial interpolations of temperature in order to interpret trends and microclimate variation across the city. After mining the data output from the HOBO stations in Excel, the week of 25-30 March 2013 was selected for further

Figure 4. Mobile sampling instrumentation: A) IR radiometer, B) Air temperature and relative humidity sensor within solar shield, and C) GPS (not shown).

analysis due to the discovery of a high magnitude UHI event on 25 March. Due to the lack of *in situ* data points (ten), it was decided that the inverse distance weighting (IDW) technique would be utilized to visualize spatial patterns in temperature over 24 hours from 1200 29 March – 1200 30 March (CDT). IDW is an interpolation technique that estimates cell values in a grid from a set of sample points that have been weighted so that the farther a sampled point is from the cell being evaluated, the less weight it has in the calculation of the cell's value (ESRI 2015). IDW is ideal for creating hotspots for areas of higher or lower value extremes, in this case, temperatures. Ordinary kriging, another interpolation technique which requires a greater amount of points for a smoother surface map, was chosen to map out mobile sampling points. Kriging weights surrounding measured values to derive a predicted value for an unmeasured location and works best with a large dataset of at least 50 points. Since mobile sampling done during the study had hundreds of data points collected every 1 second along a 20 minute driving route, kriging interpolation was ideal for mapping out air temperatures within Kingsville.

In addition to spatial interpolation, a 500 m buffer around each station was created in ArcGIS to interpret influences of upwind land surfaces on station temperature and humidity values. The buffer around each station was altered to an elliptical shape to reflect wind speeds in the prevailing wind direction. These buffers allowed for a visual analysis of the microclimatic influences on the temperature outputs of land cover upwind from the weather stations. The 500 m buffer (fetch distance) was determined to be optimal, based on scholarly literature (Schmidt 1997). Thus, during higher wind speed events, the buffer would be elongated greater than 500 m to reflect a more regional influence on the temperature, rather than a micro– or local-scale influence during calm or light wind events (i.e. < 4 m s-1).

For satellite imagery analysis, the availability of imagery from the Advanced Spaceborne Thermal Emission and Reflection Radiometer (ASTER) sensor aboard NASA's Terra satellite platform was considered. However, as discussed above, only one image from November 2012 was cloud-free and suitable for analyzing surface temperature differences. After the release of Landsat 8 imagery in May 2013, originally called the Landsat Data Continuity Mission (LDCM) during testing, we discovered two cloud-free days, one each in May and July 2013, and downloaded the data that had been collected at noon local time on both days. The remotely sensed data were imported into Exelis ENVI image processing and analysis software to convert thermal readings into °C using ENVI thermal atmospheric correction and emissivity normalization tools. Finally, the processed images were imported into ArcGIS 10.1 for further analyses of the UHI.

2.4. Temporal analysis

Since higher wind speeds tend to mitigate the UHI magnitude, additional analysis of the UHI max (ΔT u-r (max)) and wind speed (m s-1) between urban and rural stations was conducted. HOBO 6 was selected as the best representative urban site and HOBO 3 was selected as the representative rural site for comparison. HOBO 6 is located on King Avenue near 6th Street, approximating the downtown area of Kingsville with land cover principally composed of concrete, asphalt, scattered trees, minimal grass, and other pervious surface materials. HOBO 3 is located on the north end of the city, and is a rural landscape with minimal asphalt and concrete surfaces. The site is more than 1 km from urban land covers. The predicted UHI max value for a city of 27,000 is approximated by Oke (1973) at 3.5°C. UHI max reflects summertime conditions of clear skies and minimal wind speeds for cities in Quebec, Canada. This value was compared to the actual value for the study period (25-30 March 2013).

To determine the relationships between wind speeds and cloud cover, as well as their effects on temperature and UHI, multiple linear regression was used to analyze hourly wind and cloud data from the airport (KNQI), and the changes in UHI magnitude (i.e. temperature differences) between HOBO 6 (urban), and HOBO 3 (rural) during two 24-hour periods, 25-26 March 2013 (0000 to 2400 CDT) and 29-30 March 2013 (0600-0600 CDT). Typically, there is a high correlation between air temperatures, cloud coverage, and wind speeds: a higher magnitude UHI event tends to occur on days with clear skies and calm or light winds (< 4 m s-1). However, due to the proximity of Kingsville to the Gulf of Mexico, moderate easterly sea breezes develop nearly every afternoon lasting into early evening. The sea breeze, in combination with scattered clouds produced by the gulf moisture, tends to inhibit any UHI that develops in the small downtown area of Kingsville.

3. Results

3.1. Temperature interpolations

Analysis of the station data reveals that on 25 March, there was a 3.6°C UHI event in Kingsville (Figure 5). Spatial interpolations of temperatures revealed a contrasting pattern of temperature throughout the 24-hour period on 29-30 March, . First, at 1200 CDT (Figure 6a), the downtown area of Kingsville was cooler than the surrounding rural region, by as much as 2°C. It is not surprising that wind speeds at this time were minimal, averaging < 4 m s-1. A cooler downtown due to greater morning shade adjacent to a warmer rural environment due to less shade, is the inverses of the normal UHI, where the downtown is warmer than surrounding rural areas. Six hours later, at 1800 CDT, temperature differences are minimal across the study area, with a difference of less than 1°C between

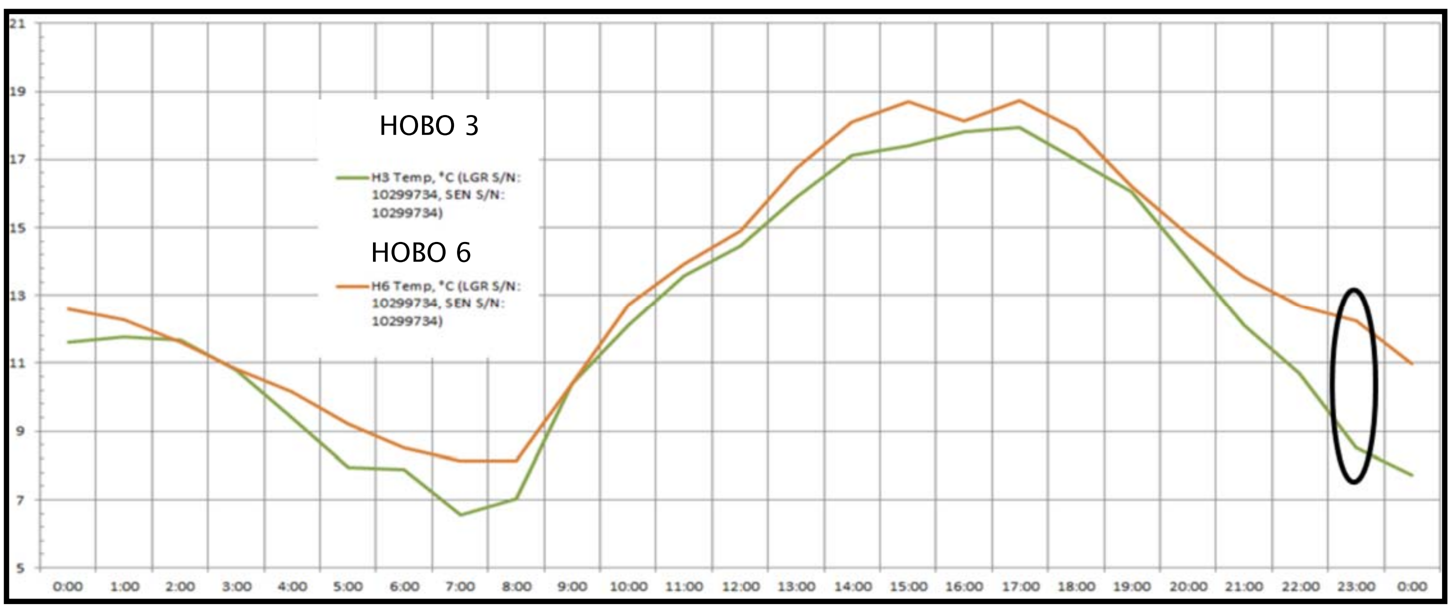

Figure 5. Comparisons of HOBO 3 (rural) and HOBO 6 (urban) on 25 March 2013. The maximum difference and heat island is indicated near the end of the day (2300 CDT). HOBO 3 recorded 8.6°C and HOBO 6 at 12.2° C, a difference of 3.6°C .

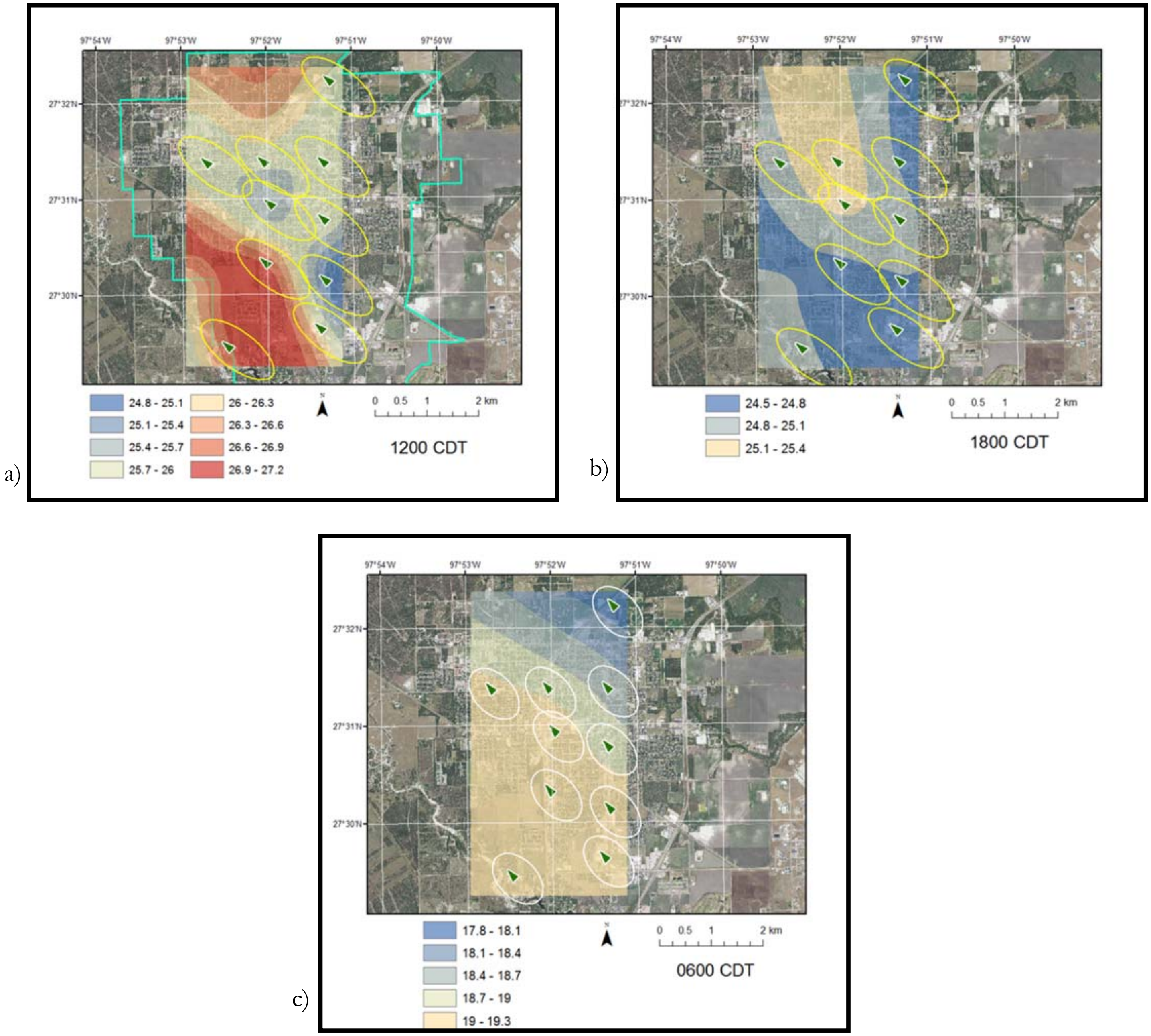

Figure 6. Temperature interpolations for the 29-30 March 2013 case study: a) 1200 29 March, b) 1800 29 March, and c) 0600 30 March (CDT). Temperature ranges are modified to illustrate spatial trends and are not standardized, shown in 0.25°C increments. Buffers indicate speed and direction by the elliptical shape of the yellow circles at the Hobo sites, larger ellipses indicate higher speeds.

downtown and surrounding rural areas near the city. The sea breeze began to develop at this time, blowing from the SE at speeds that averaged 8 m s-1. The higher wind speeds across the city produce isothermal temperatures at station level height (2.5 m) due to increasing turbulence and mixing of air across the region (Figure 6b). Finally, at 0600 CDT 30 March (Figure 6c), temperature differences have increased again between the southern portion of the city and the cooler northern area, with decreasing southeasterly winds of 2.5 m s-1.

3.2. Remote-sensed imagery

Analyses of data from ASTER from November 2012 and Landsat 8 from both May and July 2013, reveal that downtown Kingsville is cooler during the middle of the day (1200 CDT) and the rural areas, with mostly unplanted fields, possess much warmer surface temperatures; as much as 10°C higher (Figures 7-9). When analyzing surface temperature trends associated with the ASTER data acquired in November 2012, it is

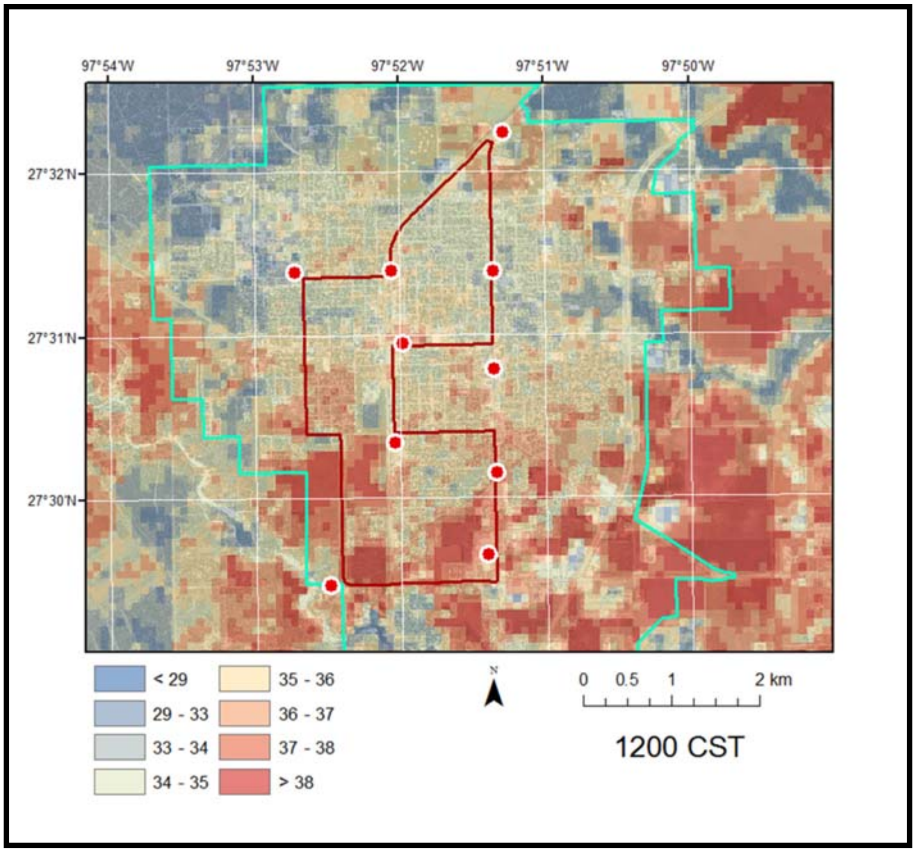

Figure 7. ASTER surface kinetic temperatures over Kingsville, Texas, acquired at 1200 CST on 8 November 2012. Temperatures are in °C. The Kingsville city boundary, mobile route, and HOBO station sites are also illustrated on the map for reference.

evident that the cooler areas (blue shading) are found along stream channels, which may contain higher moisture and/or are topographically shaded in the morning. Rural areas in the northwestern portion of the image, including a portion of the more heavily vegetated Santa Gertrudis division of the King Ranch, are also cooler than nearby agricultural fields (Figure 7). Wooded areas of the ranch would have shaded the surface in the early morning hours before the data were captured at solar noon. Synoptic weather conditions from all three dates in November, May, and July, were generally stable: clear or scattered clouds and light winds. Therefore, the maximum surface temperature differences were detected by satellite sensors on these days (Table 1).

3.3. Temporal analysis

Statistical analyses reveal some interesting diurnal patterns when comparing the KNQI Airport location (located 5.5 km southeast of downtown) to the urban site (H6) and the rural site (H3). The strongest UHI occurred when the cloud cover and wind speed were minimal (25-26 March 2013) as expected. Analysis of the weather conditions in the context of UHI during the two 24-hour periods (25 March and 30 March) revealed that both wind speed and sea level air pressure had significance above the 95% confidence level (with an R^2 at 0.36 for wind speed as a predictor of variance (25 March) and 0.73 for air pressure as a predictor (30 March)). Other variables, such as cloud cover and dew-point temperature, either failed to explain variance or exhibited multi-collinearity (Table 2). The results verify that minimal cloud cover and lower wind speeds enable stronger influences from surface land-cover properties, such as the radiative cooling contrasts between urban (i.e., concrete and asphalt composite impervious surfaces) or rural (i.e., fields with exposed pervious surfaces).

There were clear micro– or local-scale climate impacts detected by the HOBO sensors during a light – moderate wind event during the week (25-30 March 2013). Changes in the UHI during diurnal periods indicate that not only does wind speed play a role, but wind direction also influences the evening and overnight

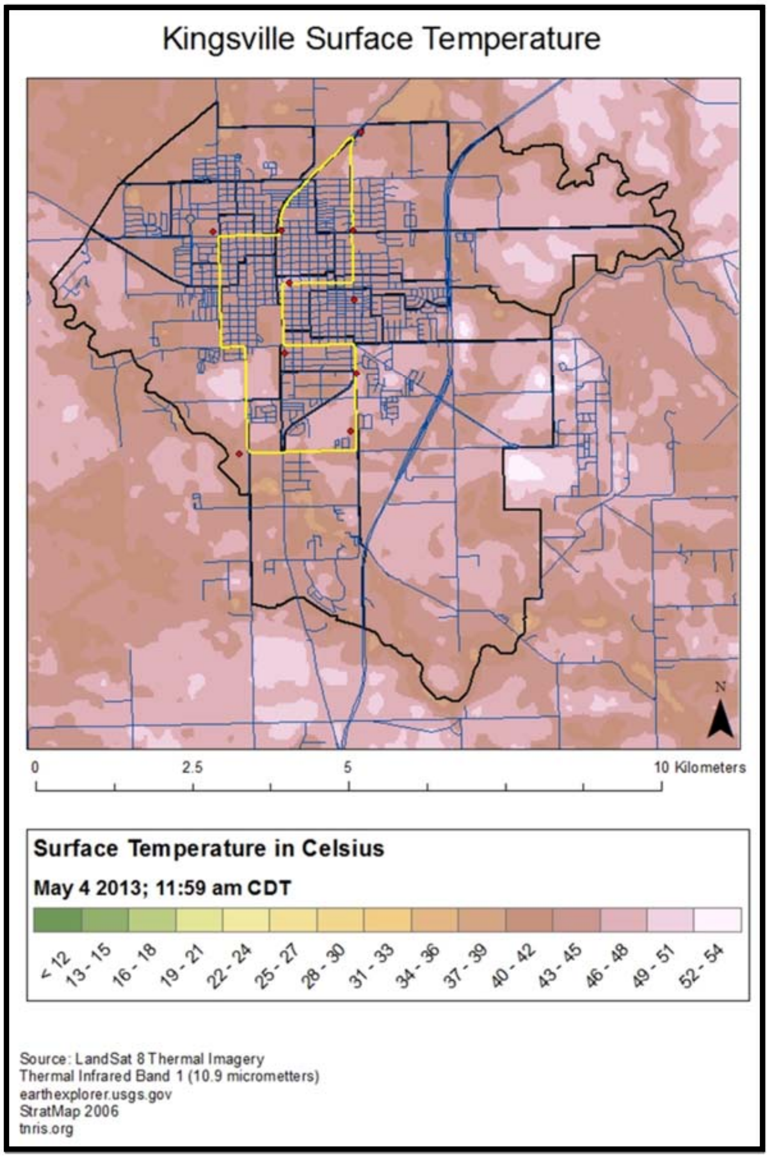

Figure 8. Landsat 8 surface kinetic temperatures over Kingsville, Texas, acquired at 1159 CDT on 4 May 2013. Note the higher temperatures over rural, unplanted farm fields, especially in the south and east of the city limits (indicated by black outline).

cooling rates at certain locations in the city. For example, H3 is influenced by the urban landscape to ~1 km to the south when the wind shifts to the southerly direction, thus transporting heat from the city core northward, which causes H3 to warm more than KNQI. However, when wind shifts to either the northerly or easterly directions, H3 is cooler than KNQI. The influences of the surface materials and their distinct properties are apparent as well when the relatively rural site KNQI is compared to (also rural) H6 when wind speed is light or calm conditions exist. As KNQI is surrounded by concrete runways and buildings, the longer wavelength radiation released from these surfaces increases air temperatures faster relative to H6 (located near fields and trees) (Table 1). The UHI magnitude (comparing H6 to H3) for the days of 25 March and 30 March averaged 0.9°C and 0.3°C, respectively. During the 24 hours leading up to the UHI max experienced at 2256 CDT on 25 March, UHI max readings were higher (>1°C) when the wind direction was from the north. With wind shifting to southerly, the UHI was generally <1°C, further substantiating the influence of wind direction and advection from urban or rural landscapes.

4. Discussion and Conclusions

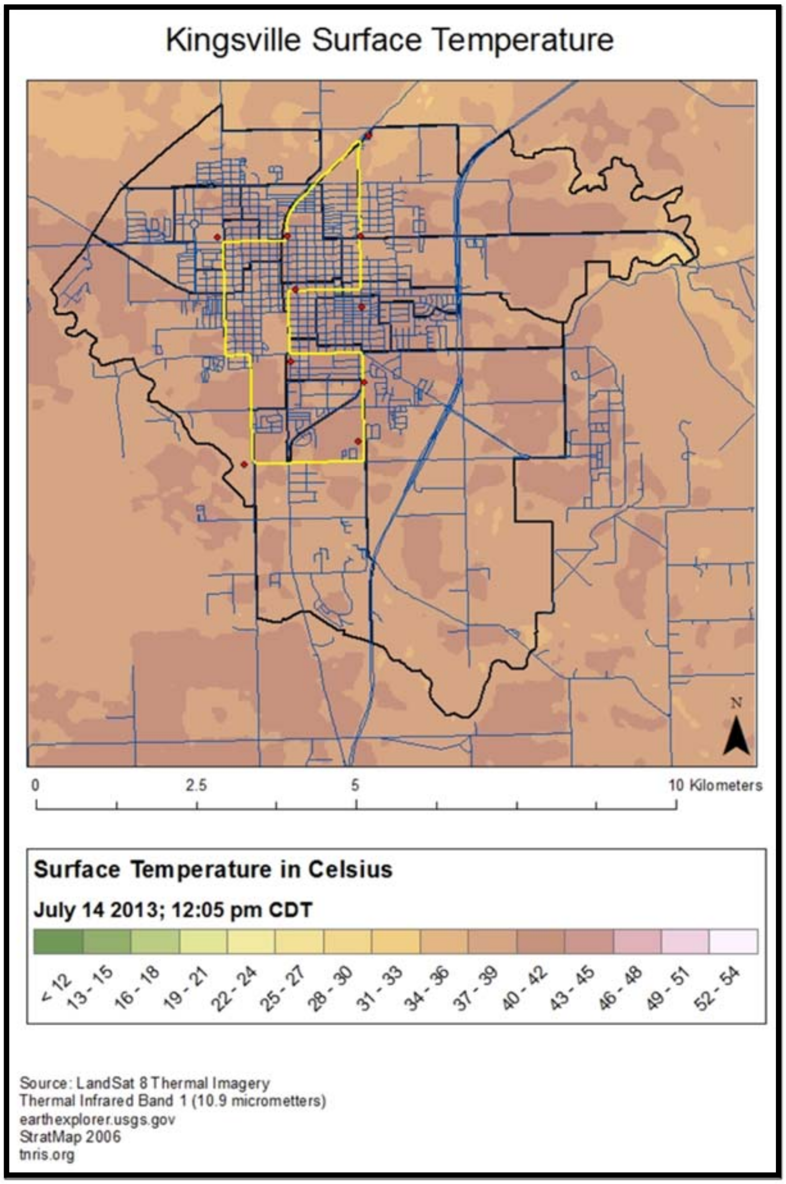

Figure 9. Landsat 8 surface kinetic temperatures over Kingsville, Texas, acquired at 1205 CDT on 14 July 2013. Surface temperatures differences are minimal.

This study confirms the existence of a moderate UHI of 3.6°C in the city of Kingsville, Texas that apparently develops during the late afternoon hours and lasts into the overnight period. The highest nighttime temperatures during UHI events occurred, as expected, primarily in the city's downtown area, but also in the most urbanized portions of city.

Urban-rural temperature differences tended to be greatest during periods of calm conditions or with light winds, but not necessarily when skies where cloudless. This corroborates a Casa Grande, Arizona UHI study (Hedquist 2005) that demonstrated that wind speed and temperature conditions were more correlated with UHI than was cloud cover. And this study also provides empirical confirmation of prior estimations of UHI maximums published by Oke (1973; 1987) that reflected city size, cloudiness, and wind conditions. The analysis performed here also detected a distinct "urban cool island" effect that developed around sunrise and persisted until about solar noon in the Kingsville region. The cool island effect resulted from rural fields absorbing and reradiating more energy, thus warming rural surface temperature faster than the more shaded urban areas. This cool island effect, which is similar to the "park cool island effect" (Chow et al. 2011), can be significant in a smaller city like Kingsville, particularly during times of drought, as was occurring during the period of this study. Presumably, more vegetation on

Table 1. Synoptic weather conditions on selected dates of data acquisition in Kingsville, Texas (KNQI).

Date[1]	Local Time	Temp. (°C)	Dew Point (°C)	Pressure (mb)	Wind (m/s)	Wind Dir. (Deg)	Cloud Cover
8-Nov-2012	1200	30.0	15.6	1018.6	7.2	135	Scattered
4-May-2013	1200	24.4	-5.0	1017.3	Calm	Calm	Clear
14-Jul-2013	1200	33.9	21.7	1012.2	3.6	155	Clear
Date[2]							
25-Mar-2013	2256	9.4	-3.9	1026.8	2.0	360	Scattered
30-Mar-2013	556	18.3	17.2	1016.9	2.6	135	Mostly Cloudy

[1]Dates of satellite image (ASTER and Landsat 8) analysis

[2]Dates of fixed station (HOBO) analysis

Table 2. Results from linear regression analysis, examining the relationship between cloud cover and wind speed on predicting the magnitude of the UHI on 25 March 2013 and 30 March 2013 in Kingsville, Texas.

Date	Dependent variable	Independent variable	F-statistic	P-values	Term coef-ficients	Sample size	R^2
25-Mar-13	UHI max	Wind speed	12.356	0.002	-3.515	24	0.36
30-Mar-13	UHI max	Air pressure	29.933	0.005	-3.147	24	0.73

fields would have reduced reradiated energy in rural areas and rural temperatures may have been moderated. Soils would also have been cooler and would be less desiccated by warm and dry conditions.

It is most likely that antecedent weather conditions (specifically a severe drought during the months prior to the data collection period in spring 2013) had an impact on surface temperatures in Kingsville, especially as many farm fields remained unplanted and soils were fairly bare. Detection of much higher daytime temperatures over fallow fields might be reason to motivate farmers to plant temporary ground cover (e.g., drought-tolerant grass or a crop), to prevent soil-desiccation due to increased temperatures. Plants would also diminish winds over the fields, slowing topsoil loss and conserving soil structure.

Recent studies conducted in Phoenix, Arizona, have demonstrated that planting trees within small geographic areas (areas smaller than a city block), can significantly lower surface temperature and can decrease the overall mean radiant temperature, increasing human comfort and reducing cooling demand within nearby (shaded) buildings (Emmanuel and Fernando 2007; Love 2009). The use of ENVI-met (Environmental Meteorology) modeling, which is a 3-D microclimate simulation model, based on the principles of thermodynamics and fluid mechanics, would provide useful simulation for assessment of the effects of tree placement for heat mitigation in future city planning (Bruse and Fleer 1998; Bruse 2015). Simulations of tree-planting scenarios in neighborhoods could be used to quantify urban forest benefits in terms of both reducing energy demand for heating and cooling and the promotion of more comfortable outdoor environments (Wang et al. 2015).

City planners and policy makers in the South Texas region ought to consider increasing the urban forest within metropolitan regions with extensive urban land cover. They should particularly strive to incorporate drought-tolerant vegetation in their landscapes. This strategy can have multiple benefits, including providing shade and comfort to pedestrians, retaining soil moisture during extended period of dry weather, and lowering pollution levels. The city of

Kingsville has recently partnered with Texas A&M University-Kingsville in this regard with two recent service-learning grant awards. These service-learning awards provided students opportunities to aid the Kingsville community by planting trees in several sections of the city.

References

Aniello, C., K. Morgan, A. Busbey, and L.Newland. 1995. Mapping micro-urban heat islands using Landsat TM and a GIS. *Computers and Geosciences* 21(8):965-969.

Arnfield, J.A. 2003. Two decades of urban climate research: a review of turbulence, exchanges of energy and water, and the urban heat island. *International Journal of Climatology* 23:1-26.

Bruse, M., and H. Fleer. 1998. Simulating surface-plant-air interactions inside urban environments with a three dimensional numerical model. *Environmental Modeling and Software* 13:373-384.

Bruse, M. 2015. The Hitchhiker's Guide to ENVI-met. http://www.model.envi-met.com/ (accessed 1 September 2015).

Chow, W.T.L., R.L. Pope, C.A. Martin, and A.J. Brazel. 2011. Observing and modeling the nocturnal park cool island of an arid city: horizontal and vertical impacts. *Theoretical and Applied Climatology* 103:197-211.

Chow, W.T.L., D. Brennan, and A.J. Brazel. 2012. Urban heat island research in Phoenix, Arizona: Theoretical contributions and policy applications. *Bulletin of the American Meteorological Society* 93: 517-30.

Debbage, N., and J.M. Shepherd. 2015. The urban heat island effect and city contiguity. *Computers, Environment and Urban Systems* 54:181-194.

Emmanuel, R., and H.J.S. Fernando. 2007. Urban heat islands in humid and arid climates: role of urban form and thermal properties in Colombo, Sri Lanka and Phoenix, USA. *Climate Research* 34:241-251.

ESRI. 2015. http://support.esri.com/en/knowledgebase/GISDictionary search/ (accessed 17 March 2015).

Geiger, R., R.H. Aron, and P. Todhunter. 2003. *The Climate near the Ground*, 6th ed. Rowman & Littlefield, Oxford.

Georgescu, M., P.E. Morefield, B.G. Bierwagen, C.P. Weaver. 2014. Urban adaptation can roll back warming of emerging megapolitan regions. *Proceedings of the National Academy of Sciences of the U.S.A.* 111(8):2909-2914.

Goward, S.N. 1981. Thermal behavior of urban landscapes and the urban heat island. *Physical Geography* 2:19-33.

Hedquist, B.C. 2002. Spatio-temporal Variation in the Phoenix East Valley Urban Heat Island. M.A. Thesis, Arizona State University, Tempe, AZ.

Hedquist, B.C. 2005. Assessment of the urban heat island in Casa Grande, Arizona. *Journal of the Arizona-Nevada Academy of Science* 38(1):29-39.

Hedquist, B.C. 2010. Microscale Evaluation of the Urban Heat Island in Phoenix, Arizona. Ph.D. Dissertation, Arizona State University, Tempe, AZ.

Love, J.M. 2009. Examining Improved Pedestrian Thermal Comfort through Urban Design. MUEP final project, Arizona State University, Tempe, AZ.

Middel, A., N. Chetri, R. Quay. 2015. Urban forestry and cool roofs: Assessment of heat mitigation strategies in Phoenix residential neighborhoods. *Urban Forestry & Urban Greening* 14:178-186.

NCDC. 2014. 1981-2010 U.S. Climate Normals. http://www.ncdc.noaa.gov/ (accessed 30 October 2014).

Oke, T.R. 1973. City size and the urban heat island. *Atmospheric Environment* 7:769-779.

Oke, T.R. 1976. The distinction between canopy and boundary-layer urban heat islands. *Atmosphere* 14:268-277.

Oke, T.R. 1982. The energetic basis of the urban heat island. *Quarterly Journal of the Royal Meteorological Society* 108:1-24.

Oke, T.R. 1987. *Boundary Layer Climates*, 2nd ed. Methuen, London.

Saaroni, H., E. Ben-Dor, A. Bitan, and O. Potchter. 2000. Spatial distribution and microscale characteristics of the urban heat island in Tel-Aviv, Israel. *Landscape and Urban Planning* 48:1-18.

Schmidt, H.P. 1997. Experimental design for flux measurements: matching scales of observations and fluxes. *Agriculture and Forest Meteorology* 87:179-200.

Stabler, L.B., C.A. Martin, and A.J. Brazel. 2005. Microclimates in a desert city were related to land use and vegetation index. *Urban Forestry & Urban Greening* 3:137-147.

Sun, C.-Y., A.J. Brazel, W.T.L. Chow, B.C. Hedquist, L. Prashad. 2009. Desert heat island study in winter by mobile transect and remote sensing techniques. *Theoretical and Applied Climatology*, 98(3): 323-335.

Sung, C.Y. 2013. Mitigating surface urban heat island by a tree protection policy: A case study of The Woodlands, Texas, USA. *Urban Forestry & Urban Greening* 12: 474-480.

Texas Trees Foundation. 2014. Benefit of trees. http://www.texastrees.org/research/benefits-of-trees/ (accessed 19 March 2015).

Unger, J., Z. Sumeghy, J. Zoboki. 2001. Temperature cross-section features in an urban area. *Atmospheric Research* 58:117-127.

U.S. Census. 2016. American FactFinder: Kingsville city, Texas. http://factfinder.census.gov/faces/nav/jsf/pages/community_facts.xhtml. (accessed 16 May 2016).

Voogt, J.A., T.R. Oke. 2003. Thermal remote sensing of urban climates. *Remote Sensing of Environment* 86: 370-384.

Wang, Y., F. Bakker, R. De Groot, H. Wortche, R. Leemans. 2015. Effects of urban trees on local outdoor microclimates: Synthesizing field measurements by numerical modelling. *Urban Ecosystems*, DOI: 10.1007/s11252-015-0447-7.